ELSEVIER

Journal of Alloys and Compounds 293–295 (1999) 552–555

Journal of ALLOYS AND COMPOUNDS

Electrochemical and structural characteristics of amorphous $MgNi_x$ ($x \geq 1$) alloys prepared by mechanical alloying

Shu G. Zhang[a], Yasutaka Hara[a], Tsutomu Morikawa[b], Hiroshi Inoue[a], Chiaki Iwakura[a,*]

[a]*Department of Applied Chemistry, Osaka Prefecture University, Sakai, Osaka 599-8531, Japan*
[b]*Technology Research Institute of Osaka Prefecture, Izumi, Osaka 594-1157, Japan*

Abstract

The hydriding and structural characteristics of amorphous $MgNi_x$ alloys prepared by mechanical alloying have been investigated with charge–discharge tests and X-ray photoelectron spectroscopy (XPS) in combination with X-ray excited Auger electron spectroscopy (XAES). It was found that the increase in Ni content lead to a significantly enhancement in cycle performance of $MgNi_x$ alloys. XPS and XAES investigations indicated the existence of a significantly thicker Ni enriched layer for the $MgNi_{1.5}$ and $MgNi_{2.0}$ alloys than that for the MgNi alloy. These results reveal that excess of Ni in $MgNi_x$ alloys may improve the cycle performance of alloy electrodes by suppressing the segregation of Mg during electrochemical cycling.

Keywords: $MgNi_x$ alloy; Amorphous; Ni–MH battery; XPS; X-ray Auger

1. Introduction

Magnesium-based hydrogen storage alloys have been considered to be possible candidates for use as the negative electrode in Ni–metal hydride batteries, due to their extremely high discharge capacity, lower specific gravity, and richer natural resources [1]. Nevertheless, the crystalline Mg_2Ni alloy can reversibly absorb and desorb hydrogen only at high temperatures, such as 250°C; while the crystalline $MgNi_2$ alloy does not absorb hydrogen at all. The research activities of many groups have therefore concentrated on lowering the hydriding temperature of Mg-based alloys [2,3].

Lei and coworkers [4,5] and our group [6,7] reported that a MgNi alloy prepared by ball-milling can charge and discharge in a Ni–metal hydride battery at room temperature, which opened a new possibility for the application of the Mg-based alloys in Ni–metal hydride batteries. Orimo et al. [8,9] reported that by ball-milling of Mg_2Ni with metallic Ni, the resultant MgNi alloy absorbed hydrogen more easily than the initial alloy. Kohno et al. [10,11] and our group [12,13] reported that amorphous alloys prepared by ball milling of Mg_2Ni with Ni exhibited discharge capacities ranging from 750 to 1086 mAh g^{-1} (Mg_2Ni). All the investigations suggest that the amorphous Mg-alloys differ greatly in nature from the crystalline ones, and Ni may play an extremely important role in facilitating the absorption and desorption of hydrogen.

On the other hand, although amorphous MgNi alloys prepared by mechanical alloying have been demonstrated to reversibly absorb and desorb hydrogen at room temperature, there has been little further investigation on the structural and electrochemical properties of the alloys containing excess of Ni. Investigations on the effect of Ni on the electrochemical behavior of MgNi alloys as well as the relation between the structural characteristics and the electrochemical hydriding properties will be vitally important for a better understanding of the electrode performance of Mg-based alloys.

In the present study, structural and electrochemical properties of $MgNi_x$ alloys with $x = 1.0 \sim 2.0$ were investigated, with the intention of revealing the role of Ni played in the microstructure and electrochemical hydriding processes.

2. Experimental

The detailed procedures for the preparation of MgNi alloy were the same as those described in the previous papers from this laboratory [6,7,12]. The prepared alloys were kept in an Ar atmosphere for charge–discharge tests and spectroscopic measurements. Preparation of the alloy

---

*Corresponding author.
E-mail address: iwakura@chem.osakafu-u.ac.jp (C. Iwakura)

0925-8388/99/$ – see front matter
PII: S0925-8388(99)00410-7

electrodes and charge–discharge tests were performed according to the same procedures as those described in our previous paper [12].

X-ray photoelectron (XPS) and X-ray excited Auger electron spectroscopy (XAES) measurements were carried out with a PHI ESCA 5700 CI spectrometer using AlK_α radiation (1486.6 eV). Ar^+ ion bombardment at 4 keV was used for depth profile measurements and SiO_2/Si was used as a reference to estimate the sputtering rates. The C 1s peak at 284.6 eV was used to calibrate the peak positions. The quantitative data were obtained using a sensitive factor method. The Ni/Mg ratios were estimated from the Ni 2p and Mg 2p peaks. Before each measurement, the brief exposure to air was strictly controlled to be the same from sample to sample, which was well comparable to the histories of the alloy electrodes for the electrochemical experiments.

3. Results and discussion

Fig. 1 shows the X-ray diffraction (XRD) patterns of the MgNi, $MgNi_{1.5}$, and $MgNi_{2.0}$ alloys. Only broad peaks at around 40–45 degree were observed, indicating that amorphous $MgNi_x$ phases were formed for MgNi, $MgNi_{1.5}$, and $MgNi_{2.0}$ alloys. Although it has been reported that the amorphous Mg_2Ni alloy cannot be prepared by mechanical alloying of Mg and Ni [14], $MgNi_x$ (x=1.0~2.0) studied here, in contrast, can readily form amorphous alloys. These results indicate that Ni plays an important role in stabilizing the amorphous phases of various $MgNi_x$ alloys with $x \geq 1$.

A minor change in the XRD band position from MgNi to $MgNi_{2.0}$ was observed, and with increase in the amount of Ni in the alloy, the XRD band shifted to the high 2θ region. This is due to the introduction of Ni which has a smaller atomic diameter than Mg.

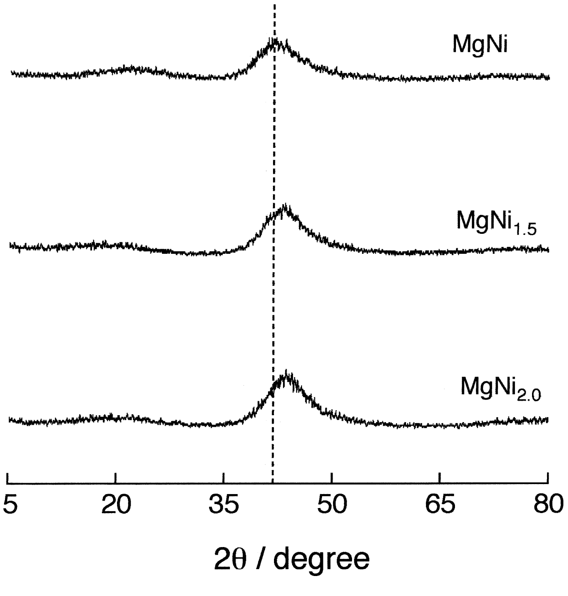

Fig. 1. The XRD patterns of the $MgNi_x$ alloys.

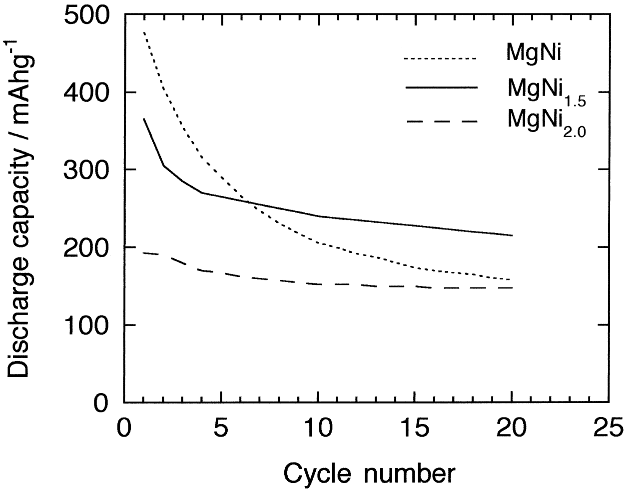

Fig. 2. Discharge capacity as a function of the cycle number for the $MgNi_x$ alloys.

Fig. 2 depicts the charge–discharge capacities of $MgNi_x$ alloys as a function of the cycle number. For all the $MgNi_x$ alloys with x=1.0~2.0, the largest discharge capacity was obtained at the first cycle, indicating that the fundamental structural characteristics of the three alloys responsible for the activation and hydriding processes may be quite similar. In the case of MgNi, comparable with the previously reported values [6,7], the maximum discharge capacity amounts to about 490 mAh g^{-1}, while for $MgNi_{1.5}$ a discharge capacity of 370 mAh g^{-1} and for $MgNi_{2.0}$ a discharge capacity of 200 mAh g^{-1} was found. A monatomic decrease in the discharge capacity was observed from MgNi to $MgNi_{2.0}$ for the first cycle. This can be attributed to the decrease of Mg amount in unit mass of alloy, and also suggests that Ni in alloys contributed little to the discharge capacity of $MgNi_x$ alloys directly.

Also from Fig. 2, another interesting feature that can be seen is that the cycle performance of either the $MgNi_{1.5}$ or the $MgNi_{2.0}$ alloy is much better than the MgNi alloy. For the $MgNi_{1.5}$ alloy, although the difference in discharge capacity from that of the MgNi alloy at the first cycle amounts to 120 mAh g^{-1}, a discharge capacity the same as that of the MgNi alloy was reached at the sixth cycle, and a higher level than the MgNi alloy was kept afterwards. At the 20th cycle, the $MgNi_{1.5}$ alloy exhibited a discharge capacity of 210 mAh g^{-1}, which was about 60 mAh g^{-1} higher than that of the MgNi alloy. In the case of the $MgNi_{2.0}$ alloy, even the difference in discharge capacity from that of the MgNi alloy was much larger at the first cycle, a similar discharge capacity to the MgNi alloy was observed at the 20th cycle. All these results suggest that the cycle life of $MgNi_x$ alloy electrodes can be greatly enhanced by increasing Ni content in alloys.

In order to understand the role of Ni played in $MgNi_x$

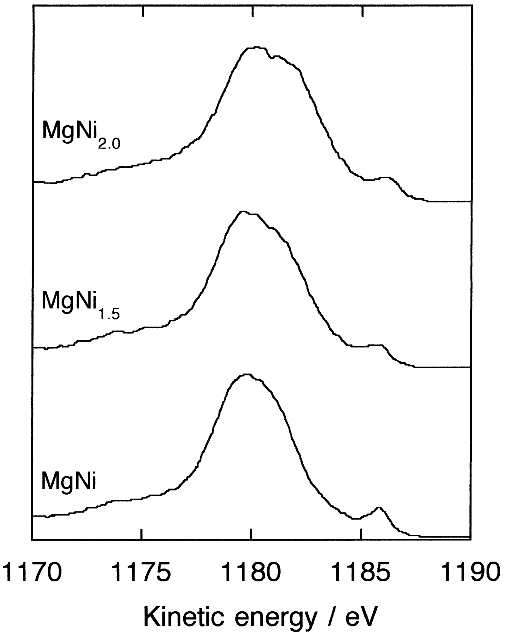

Fig. 3. Mg KLL XAES spectra observed for $MgNi_x$ alloys.

alloy electrodes, the $MgNi_x$ alloys were investigated with XPS and XAES measurements. Fig. 3 shows the Mg KLL XAES spectra observed with various $MgNi_x$ alloys. It has been found that the XAES measurement is a very useful method in distinguishing the metallic Mg from its oxide counterpart, due to the larger chemical shift in XAES than XPS [15]. For all three alloys, the band at around 1186 eV can be assigned to metallic Mg and the one at around 1181 eV to Mg oxide [16]. In the case of MgNi, magnesium oxide dominates and only a small amount of Mg occurs in the metallic state on the alloy surface, in agreement with our previous report. For $MgNi_{1.5}$ and $MgNi_{2.0}$, the relative amounts of MgO versus metallic Mg on alloy surfaces as estimated from XAES data are quite similar to that of the MgNi alloy. Minor difference in the full width at half of maximum of Mg KLL bands for alloys with different x values was most probably due to the minor changes in surface contamination. These results indicated that the chemical state of Mg is similar for all three alloys, and therefore, the difference in the cycle performances of the $MgNi_x$ alloy electrodes does not result from any difference in chemical state of Mg directly.

Fig. 4 shows the Ni 2p core level spectra observed with various $MgNi_x$ alloys. For MgNi, two strong bands appeared at 852.5 eV, 870.0 eV and another set of peaks at 855.0 eV and 875.2 eV, respectively. The former set of peaks correspond to the metallic nickel while the latter set of peaks are related to nickel oxide [17]. The strong peaks at 852.5 and 870 eV clearly indicated that Ni mainly exists in the metallic state with only a small fraction of nickel oxide existing on the surface of the MgNi alloy. In the cases of $MgNi_{1.5}$ and $MgNi_{2.0}$, the peaks due to nickel oxides become stronger than that of the MgNi alloy, and the intensity is dependent on the amount of Ni in the alloys, i.e., the more Ni, the stronger the peaks of nickel oxide. It has been reported that in a MgNi alloy, due to the extremely large oxidative affinity of Mg, Ni may be protected from being oxidizing to a certain extent by Mg, and consequently the Ni occurs mainly in the metallic state on the surface of alloy. The results obtained from the $MgNi_{1.5}$ and $MgNi_{2.0}$ alloys seem to suggest that with the increase of Ni content in alloys, the protective effect of Mg weakens.

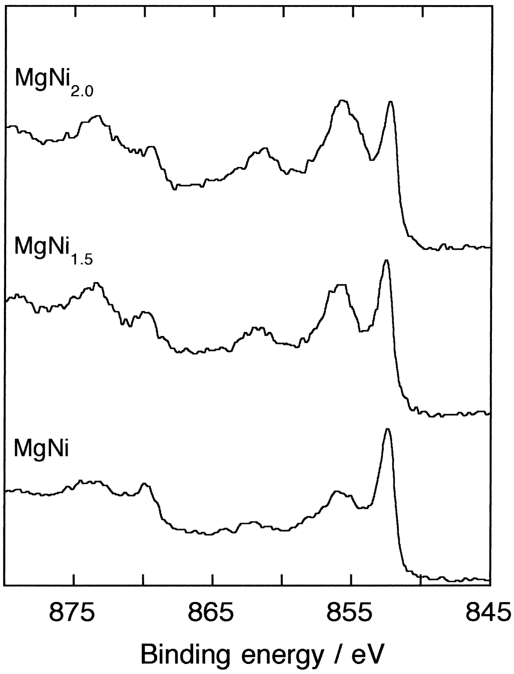

Fig. 4. Ni 2p XPS spectra observed for $MgNi_x$ alloys.

Fig. 5 depicts the depth profiles from XPS measurements for $MgNi_x$ alloys. It can be seen that upon sputtering, the Ni/Mg ratio changes dramatically with depth, indicating that the distribution of Mg and Ni in the alloy

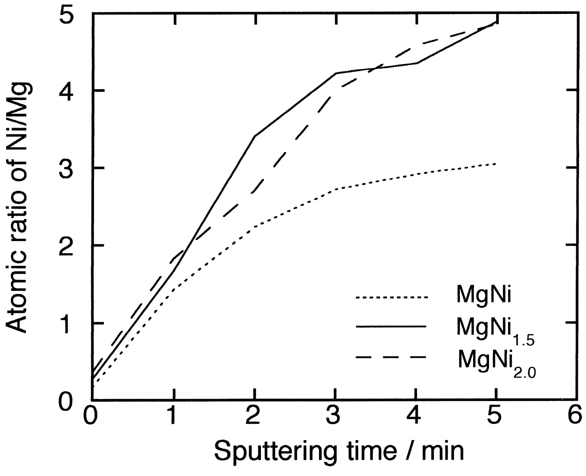

Fig. 5. XPS depth profiles for $MgNi_x$ alloys.

bulk is quite different from that on the surface. On the alloy surface, Mg dominates for all three alloys. Upon sputtering, the increase in Ni/Mg ratio for either $MgNi_{1.5}$ or $MgNi_{2.0}$ is much more rapid than that for the MgNi alloy. The Ni/Mg ratio is 2.91 for MgNi after 4-min sputtering, while it amounts to 4.34 and 4.58 for $MgNi_{1.5}$ and $MgNi_{2.0}$, respectively. The Ni/Mg ratios of both $MgNi_{1.5}$ and $MgNi_{2.0}$ are larger than that of the MgNi alloy and similar Ni/Mg ratios were maintained between the $MgNi_{1.5}$ and $MgNi_{2.0}$ alloys. Note that the cycle performances of both $MgNi_{1.5}$ and $MgNi_{2.0}$ are much better than that of the MgNi alloy; the larger Ni/Mg ratios may be responsible for the enhancement in cycle performance of the $MgNi_{1.5}$ and $MgNi_{2.0}$ alloys.

On the other hand, it has been observed that the distribution of Mg and Ni in an amorphous MgNi alloy electrode after 20 electrochemical cycles changed into the reverse of the original alloy, which indicated that the degradation of MgNi alloy electrode involved the redistribution of Mg and Ni. This fact supports the conclusion that the Ni enriched layer underneath the top surface of alloy is responsible for the enhancement in cycle performances of $MgNi_{1.5}$ and $MgNi_{2.0}$ alloys with respect to MgNi. The larger Ni/Mg ratio directly reflects the existence of a thicker Ni enriched layer in the surface region of alloys, which stabilizes the initial alloy structure during electrochemical cycling by suppressing the migration of Mg to the surface.

4. Conclusions

In summary, we have demonstrated that the cycle performance of $MgNi_x$ alloys can be significantly enhanced by increasing the x value, i.e., introduction of excess Ni in alloys. XPS and XAES investigations revealed that such an effect resulted from the increase in Ni/Mg ratio in the surface region underneath the top surface, rather than from changes in chemical states of either Mg or Ni in alloys. Also, due to the dilution of Mg in alloys, the discharge capacity decreased at the first cycle with the increase in Ni content.

Acknowledgements

This work has been supported in part by a Grant-in-Aid for Scientific Research on Priority Areas A of ‘‘New Protium Function’’ No. 10 148 102, Grant-in-Aid for Scientific Research on Priority Areas A of ‘‘Electrochemistry of Ordered Interfaces’’ No. 10 131 260, and Grant-in-Aid for Scientific Research (B) No. 09 555 273 from the Ministry of Education, Science, Sports and Culture of Japan.

References

[1] C. Iwakura, S. Hazui, H. Inoue, Electrochim. Acta 41 (1996) 471.

[2] H. Inoue, S. Hazui, S. Nohara, C. Iwakura, Electrochim. Acta 43 (1998) 2221.

[3] L. Zaluski, A. Zaluska, J.O. Stršn-Olsen, J. Alloys Comp. 217 (1995) 245.

[4] Y.Q. Lei, Y.M. Wu, Q.M. Yang, J. Wu, Q.D. Wang, Z. Phys. Chem. Bd. 183 (1994) 379.

[5] Q.M. Yang, Y.Q. Lei, C.P. Chen, J. Wu, Q.D. Wang, G.L. Lu, L.S. Chen, Z. Phys. Chem. Bd. 183 (1994) 141.

[6] C. Iwakura, S. Nohara, H. Inoue, Y. Fukumoto, J. Chem. Soc., Chem. Commun. (1996) 1831.

[7] S. Nohara, H. Inoue, Y. Fukumoto, C. Iwakura, J. Alloys Comp. 259 (1997) 183.

[8] S. Orimo, H. Fujii, T. Yoshino, J. Alloys Comp. 217 (1995) 287.

[9] S. Orimo, H. Fujii, J. Alloys Comp. 232 (1996) L16.

[10] T. Kohno, S. Tsuruta, M. Kanda, J. Electrochem. Soc. 143 (1996) L198.

[11] T. Kohno, M. Kanda, J. Electrochem. Soc. 144 (1997) 2343.

[12] S. Nohara, N. Fujida, S.G. Zhang, H. Inoue, C. Iwakura, J. Alloys Comp. 267 (1998) 76.

[13] C. Iwakura, H. Inoue, S.G. Zhang, S. Nohara, J. Alloys Comp. 270 (1998) 142.

[14] J. Huot, E. Akiba, T. Takada, J. Alloys Comp. 231 (1995) 815.

[15] S.G. Zhang, K. Yorimitsu, S. Nohara, T. Morikawa, H. Inoue, C. Iwakura, J. Alloys Comp. 270 (1998) 123.

[16] C.D. Wagner, P. Biloen, Surf. Sci. 35 (1973) 82.

[17] K.S. Kim, N. Winograd, Surf. Sci. 43 (1970) 625.